American Mineralogist, Volume 66, pages 185–195, 1981

A new cation ordering pattern in amesite-$2H_2$

CYNTHIA S. ANDERSON AND S. W. BAILEY

Department of Geology and Geophysics, University of Wisconsin–Madison
Madison, Wisconsin 53706

Abstract

The crystal structure of amesite-$2H_2$ from the Saranovskoye chromite deposit, North Urals Mountains, USSR, was refined in space group $C1$ to a residual of 5.7% with 1719 independent reflections. The study was undertaken to resolve conflicting interpretations of the optics, twinning, and infrared spectra of amesite from the Urals relative to data reported previously for amesite from Antarctica. There is nearly complete ordering of tetrahedral and octahedral cations in the Urals specimen, but the pattern of ordering differs from that found for the same polytype of amesite from Antarctica. Tetrahedral ordering of Si,Al in the Urals specimen preserves the identity of the ideal space group $P6_3$, but octahedral ordering of Mg,Al lowers the symmetry to $P1$. Tetrahedra lying on the pseudo-6_3 axis are all Si-rich. Octahedral Al is in the B site of each layer, but the degree of octahedral order is slightly different in the two layers. Local charge balance between adjacent layers is achieved by localization of all tetrahedral and octahedral Al in spirals around lines that parallel the Z axis and are spaced at intervals of $(a + b)/2$. We postulate that the presence, pattern, and degree of ordering can account for the observed sector and polysynthetic twinning, for differences in the bonding and geometry at the two interlayer junctions, and for the slightly triclinic shape of the unit cell. The possibility of other ordering patterns is examined. The normal assumption that all crystals of the same mineral or the same polytype have the same ordering pattern, crystallization conditions being similar, is not necessarily valid.

Introduction

This study was undertaken because of conflicting evidence as to the likelihood of cation ordering in amesite-$2H_2$ from the Saranovskoye chromite deposit in the North Urals Mountains, USSR. Hall and Bailey (1979) cite the biaxial optical nature and sector twinning of the Urals amesite as evidence of lower symmetry than the ideal space group of $P6_3$. They attribute this reduction in symmetry to cation ordering by analogy with amesite-$2H_2$ from Antarctica, which they determined by structural refinement to have nearly complete ordering of tetrahedral and octahedral cations. Serna *et al.* (1977), however, concluded that the Urals amesite was disordered on the basis of their study of the infrared patterns of a series of synthetic and natural amesites. Hall and Bailey point out one difference in the two samples that may be significant. The Urals crystals are twinned in more complex patterns than the Antarctic crystals, in that polysynthetic twin lamellae parallel to the (010) prism edges are present in some crystals in addition to the ubiquitous 6-fold sector twins on (001). They suggest that the difference in twinning may result from a difference in ordering patterns in the two samples, rather than from the presence or absence of ordering.

Preliminary examination of 30 crystals from the Urals sample (NMNH #103312) indicates that several polytypes are present. The $2H_2$ polytype is most abundant, but $6R_2$, $6R_1$, and $2H_1$ polytypes also are present (terminology of Bailey, 1969, and of Hall *et al.*, 1976). X-ray photographs reveal that some crystals have a disordered stacking of layers, in that the $k \neq 3n$ reflections appear as coalesced streaks and not as individual spots. All crystals examined with crossed nicols under the petrographic microscope are noticeably biaxial and twinned.

The $2H_2$ polytype has alternating interlayer shifts of $-b/3$ and $+b/3$ and alternating occupancy of the I and II sets of octahedral positions in successive layers (equivalent to 180° rotations). Steinfink and Brunton (1956) studied amesite-$2H_2$ from Saranovskoye. They attributed the biaxial nature to strain, and assumed the ideal hexagonal symmetry of $P6_3$ in their refinement. With this assumption, they determined the cat-

0003–004X/81/0102–0185$02.00

ion distribution to be random. The present refinement assumes triclinic symmetry.

Experimental

An untwinned sector was excised from a crystal of amesite-$2H_2$ that showed sector twinning without polysynthetic lamellae. The shape of this sector approximates a parallelogram with sides 0.25 × 0.5mm and thickness 0.08 mm. An electron microprobe analysis gives a structural formula $(Mg_{1.936}Al_{0.943}Fe^{2+}_{0.025}Cr_{0.074}\square_{0.022})(Si_{1.027}Al_{0.973})O_5(OH)_4$ on the basis of seven formula oxygens.

Although the ideal space group of $P6_3$ is hexagonal, the intensity distribution on X-ray photographs shows that the true symmetry is triclinic. The structure was refined using an orthohexagonal cell of space group $C1$. This is the same space group used by Hall and Bailey (1979) in their study of amesite from Antarctica. The true X and Y directions were picked as being parallel to the optical extinction directions on (001). Unit-cell dimensions were obtained by least-squares refinement of 15 low- to medium-angle reflections on an automated single crystal diffractometer. The refined values are $a = 5.307(1)$, $b = 9.195(2)$, $c = 14.068(3)$Å, $\alpha = 90.09(2)°$, $\beta = 90.25(2)°$, and $\gamma = 89.96(2)°$.

Data were collected on a Syntex $P2_1$ automated single-crystal diffractometer using monochromatic Mo$K\alpha$ radiation. The $2\theta:\theta$ variable scan mode was used to collect 1719 independent reflections, averaged over all octants out to $2\theta = 60°$. Crystal and electronic stability were checked after every 50 reflections by monitoring a standard reflection. Reflections were considered as observed if $I > 2\sigma(I)$ where I was calculated from $I = [S-(B_1+B_2)/B_r]T_r$, S being the scan count, B_1 and B_2 the background, B_r the ratio of background time to scan time, and T_r the 2θ scan rate in degrees per minute. Values of $\sigma(I)$ were calculated from standard counting statistics. Integrated intensities were corrected for Lp and absorption factors.

Refinement

The structure of amesite from Antarctica (Hall and Bailey, 1979) was used as the starting point for a least-squares refinement of the data. The tetrahedral cation T(1) was kept stationary in order to fix an origin in this non-centrosymmetric structure. The sense of the Z axis was determined by comparison of observed and calculated structure amplitudes. A few cycles of refinement indicated that the ordering patterns for the two amesites are different, and the scattering factors for the cation sites were adjusted appropriately. Repeated cycles of refinement, using sigma weights and varying only the positional atomic coordinates, reduced the residual to $R_1 = 11.8\%$.

At this point, four of the eight hydrogen atoms were located successfully by use of difference electron density maps. The hydrogen atoms were recognized as spherical volumes of excess electron density, representing ⅓ to ½ electrons, situated near predicted locations.

Continued refinement, varying first isotropic B values and later anisotropic B values for all atoms except hydrogen, reduced the residual to $R_1 = 6.1\%$. The remaining four hydrogen atoms then were located successfully by means of difference electron density maps. Weissenberg photographs were taken of levels that contained reflections whose observed intensities were significantly different from the calculated intensities. Data for six reflections were discarded because the photographs indicated that the observed intensities might be incorrect due to overlap by significant white radiation streaks.

Further least-squares refinement, initially varying the hydrogen atom locations and then varying the positional atomic coordinates for all the atoms along with the anisotropic B values for all but the hydrogen atoms, produced a final weighted residual of 5.7% (4.9% unweighted). The central hydrogen atom H(1) moved unreasonably close (0.4Å) to its OH(1) host, and was held constant during the final least-squares cycles at the position indicated by the difference electron density map. The other central hydrogen atom H(11) moved to within 0.7Å of its OH(11) host during refinement. This position also is suspect, but was retained for bond length calculations.

Final difference electron density maps were flat at the sites of all atomic coordinates, but had small peaks nearby that might be due to slight anisotropic β misfit. Scattering factors from the *International Tables for X-ray Crystallography* appropriate for 50% ionization were used throughout the refinement process. Fortran programs ORFLS, SHELLS, and ORFFE were used for the refinement and the determination of structural parameters and errors. The experimental data,[1] final atomic coordinates, bond lengths, thermal ellipsoid orientations,[1] and other important

[1]Tables 1 and 4 of observed and calculated structure amplitudes and of thermal ellipsoid orientations may be obtained by ordering document AM-81-146 from the Business Office, Mineralogical Society of America, 2000 Florida Avenue, N. W., Washington, D. C. 20009. Please remit $1.00 in advance for the microfiche.

Table 2. Final atomic coordinates for amesite-$2H_2$ from Saranovskoye

Atom	x	y	z	B_{equiv}	β_{11}	β_{22}	β_{33}	β_{12}	β_{13}	β_{23}
T(1)	0	0	0.0410	1.27	0.0136(7)	0.0035(2)	0.0014(1)	0.0013(3)	0.0003(2)	-0.0001(1)
T(2)	0.0023(5)	0.3339(3)	0.0425(2)	1.24	0.0122(7)	0.0031(2)	0.0016(1)	0.0008(3)	0.0005(2)	-0.0002(1)
T(11)	0.0136(4)	0.0058(2)	0.5410(1)	1.29	0.0137(6)	0.0031(2)	0.0016(1)	0.0012(3)	0.0003(2)	-0.0001(1)
T(22)	0.5073(5)	0.1709(3)	0.5424(2)	1.23	0.0139(7)	0.0032(2)	0.0013(1)	0.0006(3)	0.0001(2)	-0.0001(1)
M(1)	0.1695(5)	0.1683(3)	0.2377(2)	1.19	0.0115(7)	0.0032(2)	0.0015(1)	0.0004(3)	0.0005(2)	0.0000(1)
M(2)	0.6698(5)	-0.0031(3)	0.2374(2)	1.44	0.0135(6)	0.0039(2)	0.0018(1)	0.0008(3)	0.0002(2)	-0.0001(1)
M(3)	0.6763(5)	0.3335(3)	0.2377(2)	1.17	0.0116(7)	0.0031(2)	0.0015(1)	0.0010(3)	0.0003(2)	-0.0002(1)
M(11)	0.3434(5)	0.3400(3)	0.7380(2)	1.25	0.0125(7)	0.0031(2)	0.0016(1)	0.0008(3)	0.0001(2)	-0.0003(1)
M(22)	0.3433(5)	0.0115(3)	0.7367(2)	1.23	0.0132(6)	0.0030(2)	0.0015(1)	0.0004(3)	0.0002(2)	0.0000(1)
M(33)	0.8372(5)	0.1750(3)	0.7381(2)	1.28	0.0130(7)	0.0032(2)	0.0016(1)	0.0012(3)	0.0002(2)	-0.0001(1)
O(1)	-0.0047(10)	-0.0019(5)	0.1585(4)	1.87	0.022(2)	0.0059(5)	0.0014(2)	0.0020(7)	-0.0002(5)	-0.0002(2)
O(2)	0.0066(9)	0.3351(5)	0.1659(3)	1.42	0.015(2)	0.0040(5)	0.0016(2)	0.0015(6)	0.0001(4)	0.0000(2)
O(3)	0.0768(9)	0.1603(5)	0.0025(3)	1.69	0.018(2)	0.0037(4)	0.0022(2)	0.0008(7)	0.0009(5)	-0.0004(2)
O(4)	0.7228(8)	-0.0422(5)	0.0005(3)	1.63	0.014(2)	0.0048(5)	0.0022(2)	0.0000(7)	0.0001(4)	0.0003(3)
O(5)	0.7027(8)	0.3827(5)	0.0023(3)	1.48	0.013(2)	0.0036(4)	0.0022(2)	0.0016(6)	-0.0002(4)	-0.0003(2)
O(11)	0.0274(9)	0.0092(5)	0.6582(4)	1.48	0.016(2)	0.0044(5)	0.0014(2)	0.0013(7)	0.0004(4)	0.0001(2)
O(22)	0.4979(9)	0.1657(5)	0.6659(3)	1.43	0.015(2)	0.0040(5)	0.0015(2)	0.0002(7)	0.0003(4)	-0.0001(2)
O(33)	0.2862(9)	0.0478(5)	0.4983(3)	1.60	0.014(2)	0.0044(5)	0.0022(2)	0.0007(7)	0.0001(4)	-0.0010(2)
O(44)	0.4330(9)	0.3447(5)	0.5036(3)	1.63	0.018(2)	0.0036(4)	0.0021(2)	0.0018(7)	-0.0010(5)	0.0002(2)
O(55)	0.8071(9)	0.1229(5)	0.5031(3)	1.57	0.015(2)	0.0039(5)	0.0022(2)	0.0024(6)	0.0009(4)	0.0000(2)
OH(1)	0.5071(10)	0.1607(6)	0.1656(4)	2.17	0.025(2)	0.0078(6)	0.0014(2)	0.0000(8)	0.0005(5)	-0.0003(3)
OH(2)	0.3447(11)	0.0004(6)	0.3062(4)	2.01	0.023(2)	0.0066(6)	0.0015(2)	-0.0033(8)	0.0010(5)	-0.0004(3)
OH(3)	0.3388(10)	0.3373(6)	0.3071(4)	1.76	0.024(2)	0.0042(5)	0.0015(2)	0.0014(7)	0.0000(5)	0.0002(3)
OH(4)	0.8345(10)	0.1594(6)	0.3067(4)	2.05	0.014(2)	0.0101(7)	0.0014(2)	0.0027(8)	0.0009(5)	0.0005(3)
OH(11)	-0.0009(10)	0.3523(5)	0.6659(4)	1.72	0.020(2)	0.0051(5)	0.0014(2)	0.0014(7)	0.0001(5)	0.0002(3)
OH(22)	0.6859(9)	0.3562(5)	0.8057(4)	1.59	0.016(2)	0.0051(5)	0.0016(2)	0.0003(7)	0.0005(5)	-0.0006(3)
OH(33)	0.6573(10)	0.0078(5)	0.8074(4)	1.56	0.018(2)	0.0042(5)	0.0015(2)	0.0003(7)	-0.0001(5)	0.0002(3)
OH(44)	0.1815(10)	0.1651(5)	0.8070(4)	1.64	0.021(2)	0.0042(5)	0.0014(2)	0.0020(7)	0.0005(5)	-0.0004(3)
H(1)*	0.507	0.156	0.104	2.00						
H(2)	0.304(16)	0.037(9)	0.365(7)	2.00						
H(3)	0.362(16)	0.346(9)	0.365(7)	2.00						
H(4)	0.818(16)	0.133(9)	0.368(7)	2.00						
H(11)	0.982(15)	0.387(9)	0.624(6)	2.00						
H(22)	0.689(15)	0.382(9)	0.869(6)	2.00						
H(33)	0.677(16)	0.962(9)	0.863(7)	2.00						
H(44)	0.145(16)	0.151(9)	0.871(7)	2.00						

*Position obtained from difference electron density map only.

structural features are reported in Tables 1 through 5.

Cation ordering

The final bond lengths (Table 3) indicate that ordering occurs in both tetrahedral and octahedral cation sites. Octahedral ordering reduces the symmetry from $P6_3$ to $P1$ (or $C1$ as oriented here). In the ideal hexagonal space group there are two unique tetrahedra in each layer, which are related to equivalent tetrahedra in adjacent layers by a 6_3 axis. These hexagonally equivalent tetrahedral sites are identical in adjacent layers of this amesite, thus preserving the identity of the 6_3 axis so far as the tetrahedral compositions are concerned. Tetrahedra lying on the 6_3 axis are all Si-rich. Of the three octahedral sites in each layer, one is smaller than the other two and is interpreted as Al-rich. In the ideal hexagonal space group, the three octahedra are equivalent to one another by a 3-fold rotation axis parallel to Z. Octahedral ordering violates this equivalence, thereby reducing the symmetry to $P1$. If the 180° rotation of the second layer relative to the first layer is taken into account, it can be seen that the smaller, Al-rich octahedron is in the same relative position in each layer (Fig. 1). The layers are not identical, however, since bond lengths indicate that the degree of octahedral ordering is greater in the second layer than in the first layer. Note that this ordering pattern contrasts with that of amesite from Antarctica, even though both specimens are of the $2H_2$ polytype. Hall and Bailey (1979) report for Antarctic amesite that Si and Al alternate in adjacent layers along vertical lines through the lattice points, thus violating the 6_3 axes of the ideal space group, and that octahedral Al is located in different relative positions in each layer. No difference in the degree of ordering between the two layers was noted for the amesite from Antarctica.

Mean T–O values of 1.629, 1.740, 1.630, and 1.740Å indicate that ordering of Si and Al in the tetrahedral sites is substantial but incomplete. Hall and Bailey present an equation relating mean T–O bond lengths to Si,Al compositions for 1:1 layer silicates. The equation was derived, in part, from results ob-

Table 3. Calculated bond lengths (Å) and angles

	to T(1)		to T(2)		to T(11)		to T(22)
O(1)	1.653(6)	O(2)	1.736(5)	O(11)	1.652(5)	O(22)	1.740(5)
O(3)	1.624(5)	O(3)	1.738(5)	O(33)	1.616(5)	O(33)	1.742(5)
O(4)	1.622(5)	O(4)	1.740(5)	O(44)	1.628(5)	O(44)	1.735(5)
O(5)	1.618(4)	O(5)	1.744(5)	O(55)	1.625(5)	O(55)	1.743(5)
Mean	1.629	Mean	1.740	Mean	1.630	Mean	1.740

	in T(1)	in T(2)		in T(11)	in T(22)
O(ap)-O(3)	2.692(7)	2.829(6)	O(ap)-O(33)	2.666(7)	2.822(6)
O(4)	2.672(7)	2.835(6)	O(44)	2.693(7)	2.837(6)
O(5)	2.679(7)	2.839(6)	O(55)	2.685(7)	2.850(6)
O(3)--O(4)	2.646(6)	2.844(6)	O(33)-O(44)	2.648(6)	2.841(6)
O(5)	2.638(6)	2.850(6)	O(55)	2.636(6)	2.850(6)
O(4)--O(5)	2.638(6)	2.846(6)	O(44)-O(55)	2.643(6)	2.846(5)
Mean	2.661	2.841	Mean	2.662	2.841

Interlayer Contact			O(H)..H Bond	∠ OH-H to (001)	Angle OH-H..O_b	H..O_b Bond
OH(2)-O(33)	2.757(7)	H(2)	0.92(9)	64.1°	158.3°	1.88(10)
OH(3)-O(44)	2.807(7)	H(3)	0.83(10)	79.9°	173.6°	1.98(10)
OH(4)-O(55)	2.788(7)	H(4)	0.90(9)	73.4°	166.9°	1.90(10)
Mean	2.784	H(1)	0.87(-)			1.92
OH(22)-O(5)	2.777(7)	H(22)	0.91(9)	75.3°	165.5°	1.88(9)
OH(33)-O(4)	2.776(7)	H(33)	0.90(9)	61.1°	153.2°	1.94(10)
OH(44)-O(3)	2.808(7)	H(44)	0.93(9)	71.8°	166.3°	1.89(10)
Mean	2.787	H(11)	0.68(9)			1.90

	to M(1)	to M(2)	to M3)		to M(11)	to M(22)	to M(33)
O(1)	2.130(6)	2.058(6)	2.110(6)	O(11)	2.157(5)	2.004(5)	2.146(5)
O(2)	2.029(5)	1.991(5)	2.027(5)	O(22)	2.066(5)	1.921(5)	2.065(5)
OH(1)	2.063(6)	2.008(6)	2.085(6)	OH(11)	2.090(5)	1.954(5)	2.108(5)
OH(2)	2.042(6)	1.982(6)	2.018(5)	OH(22)	2.054(5)	1.921(5)	2.080(5)
OH(3)	2.041(5)	1.978(5)	2.044(6)	OH(33)	2.076(5)	1.937(5)	2.059(5)
OH(4)	2.031(5)	1.984(6)	2.050(6)	OH(44)	2.069(5)	1.927(5)	2.067(5)
Mean	2.056	2.000	2.056	Mean	2.085	1.944	2.088

	in M(1)	in M(2)	in M(3)		in M(11)	in M(22)	in M(33)
O(1)---O(2)	3.102(6)	2.999(6)	3.100(6)	O(11)---O(22)	3.164(6)	2.885(6)	3.158(6)
OH(1)	3.102(7)	2.993(7)	3.104(7)	OH(11)	2.156(6)	2.890(6)	3.160(6)
O(2)--OH(1)	3.102(6)	2.994(6)	3.099(6)	O(22)--OH(11)	3.154(6)	2.882(6)	3.166(6)
OH(2)-OH(3)	3.098(6)	3.020(7)	3.076(6)	OH(22)-OH(33)	3.131(6)	2.865(6)	3.208(6)
OH(4)	3.076(6)	2.983(6)	3.137(7)	OH(44)	3.203(6)	2.840(6)	3.162(6)
OH(3)-OH(4)	3.138(7)	2.962(7)	3.097(6)	OH(33)-OH(44)	3.153(6)	2.910(6)	3.136(7)
Mean unshared	3.103	2.992	3.102	Mean unshared	3.160	2.879	3.165
O(1)--OH(2)	2.779(8)	--	2.779(8)	O(11)--OH(22)	2.642(7)	2.642(7)	--
OH(3)	--	2.697(7)	2.697(7)	OH(33)	2.880(7)	--	2.880(7)
OH(4)	2.698(8)	2.698(8)	--	OH(44)	--	2.661(7)	2.661(7)
O(2)--OH(2)	--	2.636(7)	2.636(7)	O(22)--OH(22)	2.812(6)	--	2.812(6)
OH(3)	2.651(7)	2.651(7)	--	OH(33)	--	2.604(7)	2.604(7)
OH(4)	2.720(7)	--	2.720(7)	OH(44)	2.606(7)	2.606(7)	--
OH(1)-OH(2)	2.617(7)	2.617(7)	--	OH(11)-OH(22)	--	2.581(7)	2.581(7)
OH(3)	2.720(7)	--	2.720(7)	OH(33)	2.586(7)	2.586(7)	--
OH(4)	--	2.632(7)	2.632(7)	OH(44)	2.799(7)	--	2.799(7)
Mean shared	2.698	2.655	2.697	Mean shared	2.721	2.613	2.723

tained in their study of amesite from Antarctica. By averaging pertinent results from the present study with those from Hall and Bailey, the linear equation was modified to $\overline{T\text{–}O} = 1.619\text{Å} + 0.14\ [x_{Al}/(x_{Al} + x_{Si})]$. This equation gives values for Al^{IV} of 0.07, 0.86, 0.08, and 0.86 respectively for T(1), T(2), T(11), and T(22). The microprobe composition indicates that maximum ordering should result in tetrahedral Al values of 0.00 and 0.97.

Bond lengths suggest that the degree of octahedral

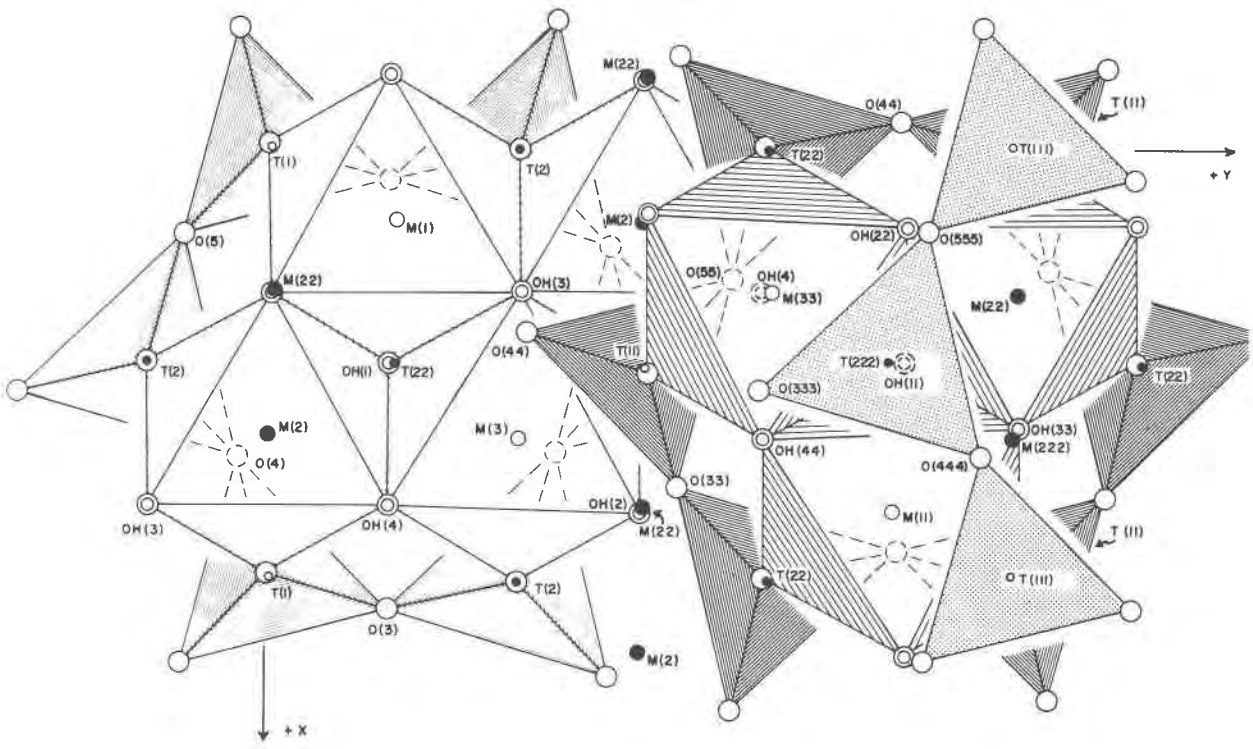

Fig. 1. Diagrammatic view of amesite-$2H_2$ structure from Saranovskoye. For clarity, the structure is cut away so that layer 1 is shown on the left side and layer 2 on the right with the bases of three tetrahedra (stippled pattern) from layer 3 superimposed. All the Al cations are shown (solid circles), some without their enclosing polyhedra. Note that each group of four unique Al atoms [T(2), M(2), T(22), and M(22)] forms a diamond in projection onto the XY plane.

ordering is different in the two layers. Mean M–O,OH values for M(1), M(2), and M(3) of the first layer are 2.056, 2.000, and 2.056Å respectively, whereas these values for M(11), M(22), and M(33) of the second layer are 2.085, 1.944, and 2.088Å respectively (Table 3). The smaller M(2) and M(22) octahedra are interpreted as Al-rich, whereas the larger M(1), M(3), M(11), and M(33) octahedra are interpreted as Mg-rich. The fact that M(11) and M(33) are both larger than M(1) and M(3) along with the fact that M(22) is smaller than M(2) are interpreted to indicate that the degree of ordering is slightly greater in the second layer. The small amounts of vacancies and of Cr and Fe ions present are assumed to be distributed randomly, because difference electron density maps show no excess density preferentially concentrated in any of the octahedral sites.

Local charge balance between adjacent layers results from the ordering pattern. Si-rich tetrahedra lie along lines parallel to Z through each lattice point. Si-rich and Al-rich tetrahedra alternate around the 6-fold rings within each layer. Adjacent layers are shifted by $\pm b/3$ so that Al-rich tetrahedra in each layer project into the centers of 6-fold rings in layers above and below. After accounting for the 180° rotation of the second layer relative to the first, which is equivalent to occupation of the second set of octahedral positions, it is seen that the Al-rich octahedron of both layers is in the B position in the terminology of Bailey (1963, Fig. 1). As a consequence of the ordering pattern, the tetrahedral and octahedral Al atoms spiral upwards, in a counter-clockwise sense, around lines that parallel Z and are spaced at intervals of $a/2 + b/2$ (Fig. 2). In projection normal to (001), the Al atoms lie at the corners of a diamond (Fig. 1). Thus, from bottom to top in the $+Z$ direction, Al occupies T(2), M(2), T(22), and M(22). Interlayer local charge balance results because the tetrahedral Al of one layer, which is the source of local excess negative charge, is closely associated with the octahedral Al of the adjacent layer, which is the source of local excess positive charge. The charge balance pattern is as good as that found by Hall and Bailey for Antarctic amesite.

Hall and Bailey report that the ordering pattern of Antarctic amesite results in local charge balance because the tetrahedral and octahedral Al are located along slightly zig-zag lines that parallel X_1 in projec-

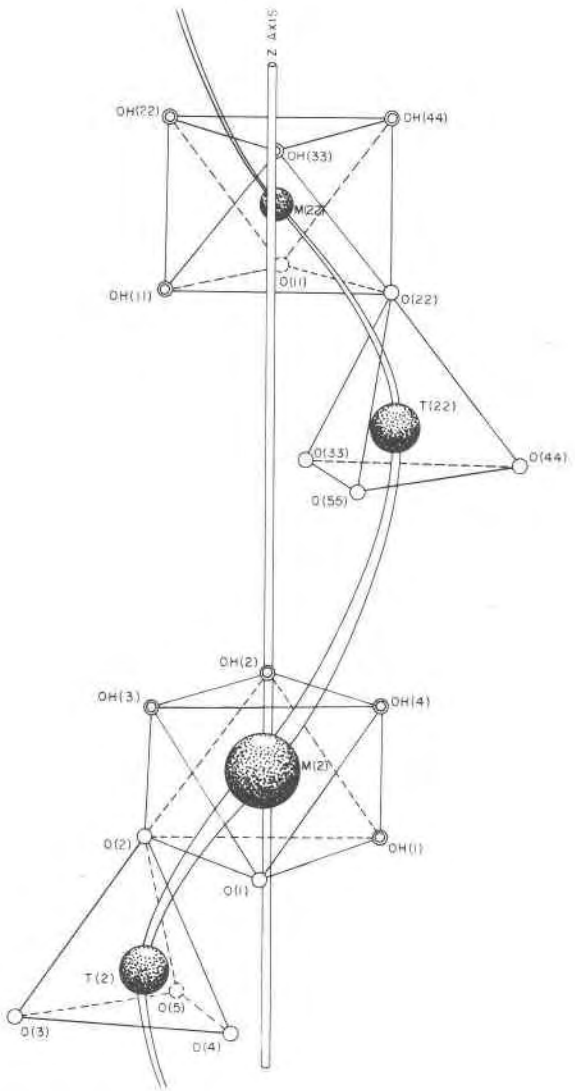

Fig. 2. Tetrahedra and octahedra enclosing Al atoms spiral along lines that parallel the Z axis. In this figure the Y axis is horizontal and lies in the plane of the page. The $+Z$ axis is tilted 10° out of the plane of the page toward the reader. The relative sizes of the Al atoms indicate distance, with M(2) closest to the reader and M(22) farthest away.

tion onto (001) and are spaced at intervals of $b/2$. Al is interpreted to occupy T(1), M(3), T(22), and M(11) in their specimen. They further show that this is not a unique ordering pattern and that six different (but geometrically similar) ordering patterns can be postulated in which lines of Al parallel the positive and negative directions of X_1, X_2, and X_3 in projection. They believe that the 6-fold sector twins, ubiquitous in their sample, result from the adoption of these six ordering patterns in the six (001) sectors. This explanation for the origin of sector twinning is reasonable in light of our results. The ordering pattern of the Saranovskoye amesite also is not unique. The pseudohexagonal nature of the structure in this case allows for a total of three similar ordering patterns in which Al spirals around lines parallel to Z. The two other ordering patterns have tetrahedral Al in the same positions as in the initial pattern [T(2) and T(22)] but differ in that octahedral Al is located either in M(1) and M(11) or in M(3) and M(33) [instead of M(2) and M(22)].

Polysynthetic twinning occurs within some of the sector twins of Urals amesite but has not been observed in amesite from Antarctica. This can be explained by the necessity to match the structures satisfactorily at the interface between two twin units. Since the Al atoms in the Antarctic amesite lie along lines that slope along six different directions in the six sectors, it is unlikely that good lateral fit could result if these sectors were arranged in the form of lamellae parallel to the (010) prism edges. In contrast, Al atoms in Urals amesite lie along vertical spirals that project onto the (001) plane in diamond shapes, and the resulting lateral distortions due to ordering are distributed more homogeneously. It is reasonable, therefore, that this amesite should exhibit more complex twinning in the (001) plane than amesite from Antarctica.

Interlayer bonding

The $2H_2$ stacking sequence of layers in this amesite results in two unique interlayer spaces that bond lengths indicate to be slightly different. In both interlayers, the basal oxygens of the upper layer move closer to the surface hydroxyls of the lower layer by means of tetrahedral twist. This results in distortion of the 6-fold rings of the tetrahedral sheets to form ditrigonal rings. The differences between the two interlayers can be explained by different degrees of octahedral ordering within the two layers.

The corrugation of the base of the layers, which is defined by the z coordinates of the basal oxygens O(3), O(4), and O(5) in the first layer and by O(33), O(44), and O(55) in the second layer, is primarily a result of octahedral ordering. The base of the second layer exhibits a more extreme corrugation than that of the first. In the second layer, octahedron M(22) is Al-rich and is smaller than M(11) or M(33). Tetrahedra T(11) and T(22) must tilt toward one another to allow their apices to form a shortened octahedral edge around M(22). This causes downward buckling of the bridging basal oxygen O(33), thus creating an irregular surface at the base of the second layer. Sim-

ilarly, M(2), the Al-rich octahedron in the first layer, causes a downward buckling of O(4). Hall and Bailey report a similar phenomenon for amesite from Antarctica, but involving different atoms because of the different pattern of ordering. The fact that O(33) of this study is relatively more depressed than O(4) is consistent with the interpretation that M(22) is more Al-rich than M(2) and thus causes greater tetrahedral tilting and downward buckling of the bridging basal oxygen. The long interlayer hydrogen bond O(33)–OH(2) of 2.757Å is thought to be especially short because O(33) is especially depressed.

There is a keying together of the two layers at the junction between the base of the second layer and the top of the first layer, whereby the lowest basal oxygen O(33) is bonded to the lowest surface hydroxyl OH(2). But the keying is not very efficient because two surface hydroxyls are depressed whereas only one basal oxygen is depressed. The junction at the top of the second layer is even less efficient. Basal oxygen O(444) at the base of the third layer is not depressed as much as is O(33), and the matching hydroxyl OH(33) on the upper surface of the second layer is not depressed at all. In the Antarctic amesite, however, both interlayers exhibit an efficient keying effect.

In Urals amesite the hydrogen protons are located at a mean distance of 0.87Å from the centers of their host hydroxyl groups, or at 0.90Å if the two suspect values for H(1) and H(11) are excluded. These values are in good agreement with similar values from the literature. The long interlayer O . . H . . . . O bonds are slightly bent, with angles ranging from 153.2° to 173.6° (Table 3). The O . . H vectors are inclined by 10°–30° from the vertical, with the largest inclination for those interlayer bonds that are most bent.

The orientations of the O . . H vectors of Urals amesite do not agree with those calculated by Giese (1980) as most stable for the Antarctic amesite. Giese found that the structure and ordering pattern of Antarctic amesite create two distinct environments for the H protons of the surface hydroxyls. The environments differ in the position of the OH relative to octahedral Al of its same layer and relative to the oxygen of the adjacent layer to which it bonds. As a result, Giese finds that the angles, ρ, between the hydroxyl O . . H bond and (001) fall into two groups—those between approximately 81° and 83° and those near 90°. Inspection of the Urals interlayers shows that the same two general H proton environments are present so that a similar grouping of ρ values might be expected. This grouping is not observed.

The discrepancies between the two sets of ρ values probably are due to two factors. First, Giese's calculations depend significantly on the exact details of the Antarctic structure, which has a different ordering pattern than that of the Urals amesite. Discrepancies of a few degrees can be expected also if the real structure is not as fully ordered as the model and if the actual O . . H distances are different than in the model (Giese, personal communication, 1980). Second, the H positions determined from refinement of the X-ray data collected for Urals amesite are necessarily imprecise. It is not reasonable to expect to locate hydrogen protons accurately with X-ray diffraction data since the protons have no scattering power of their own and are detected only as a result of their polarization of the host oxygens.

Crystallographic beta angle

In each of the two amesites studied in detail, the unit cell has a slightly triclinic shape. Most notably, both amesites have a slightly obtuse β angle (90.27° for amesite from Antarctica and 90.25° for amesite from the Urals). Comparison of the Antarctic and Urals structures with the ideal structure shows that this triclinic distortion is due to tetrahedral and octahedral ordering.

An atom-by-atom comparison of the actual and ideal structures reveals two distortions. First, the basal oxygens are seen to be displaced significantly from their positions on an ideal hexagon as a result of tetrahedral rotation. Second, there is a relative lateral displacement of the octahedral Al toward the tetrahedral Al of the same layer, but more precisely in a direction that in (001) projection is normal to the octahedral edge that contains both the apical oxygen of the Al-rich tetrahedron and the surface hydroxyl that is closest to the down-buckled basal oxygen of its own layer. For example, in the first layer of Urals amesite, Al in site M(2) is displaced along $-Y_1$, which is toward Al in site T(2) and normal to the octahedral edge O(2)–OH(3) (Fig. 1). Note that in both the Urals and Antarctic amesites the direction of movement of octahedral Al relative to tetrahedral Al is parallel in both layers of the structure.

Crystallochemically, the observed relative offset of the Al atoms is a predictable and reasonable distortion because it:

(1) draws the local excess positive charge of the octahedral sheet (due to substitution of Al^{3+} for Mg^{2+}) toward the local excess negative charge of the tetrahedral sheet (due to substitution of Al^{3+} for Si^{4+}),

(2) minimizes repulsion between the octahedral Al cation and the inner H^+ proton, and
(3) keeps the octahedral Al cation approximately equidistant from the anions of the edge toward which it moves.

The atom-by-atom comparison of the actual and ideal structures is useful in interpreting various distortions, but it is difficult to use this method to evaluate why the unit cell has a triclinic shape. Since the symmetry elements of $P6_3$ are normal to (001) and control the ideal lateral positions of all atoms, systematic offsets of atoms within planes parallel to (001) may cancel out to produce no net offset for the entire plane. Such systematic offsets of atoms (*e.g.* tetrahedral rotation to form ditrigonal rings) will not change the shape of the unit cell. Therefore, it is necessary to consider the net displacement of all atoms that ideally lie at the same z height.

To obtain a measure of the net displacement of the planes of atoms in amesite, the coordinates of the centroid for atoms that ideally lie at the same z height were determined and compared to the coordinates of the ideal centroid. In this manner, a single point can be assigned to each of the ten planes of atoms that make up the unit cell. The ten planes are those of the basal oxygen, tetrahedral cation, apical oxygen and inner hydroxyl, octahedral cation, and surface hydroxyl atoms in each of the two layers of the structure. Comparison of the actual and ideal centroids reveals that the greatest offsets occur between layers in both structures, although smaller offsets also occur within layers. Offsets within and between layers are considered separately below.

Offsets within layers

Mention has been made previously of both (1) tilting of tetrahedra to form a shortened octahedral edge around the small Al-rich cations and (2) lateral displacement of octahedral Al toward tetrahedral Al of the same layer. The centroid analysis shows that these factors have combined to produce a small net offset of the tetrahedral and octahedral sheets within the layer, which shows up as a clear separation of the differences of the observed centroids from their ideal values for the basal oxygens and tetrahedral cations relative to those of the octahedral cations, apical oxygens plus inner hydroxyl, and surface hydroxyls. The amount of this net offset can be correlated with the degree of octahedral ordering. Both the degree of octahedral ordering and the amount of offset are similar in the two layers of Antarctic amesite and in the second layer of Urals amesite. On the other hand, the amount of offset in the first layer of Urals amesite, as well as its degree of octahedral ordering, is less than in the other layers.

Offsets between layers

In both structures, there is one major and one minor interlayer offset. The minor offset is about two-thirds the magnitude of the major offset. The major offset occurs between the first and second layers of the Antarctic amesite, but between the second and third layers of the Urals amesite.

The major interlayer offset is along $-X_1$ and $-X_3$ in the Antarctic and Urals amesites, respectively. In both structures, this offset approximately parallels the line that contains the (001) projections of the octahedral Al cation and the particular surface hydroxyl bonded to the basal oxygen that projects onto the Al-rich octahedron. The direction of movement is toward the surface hydroxyl. For example, in Antarctic amesite, the offset of the second layer is towards OH(3) along the line M(3)–OH(3) (Fig. 3).

The directions of the major interlayer offsets appear to be related to the octahedral ordering patterns. Giese (1980) points out that the octahedral Al^{3+} should repel the H^+ protons of the surface hydroxyls and thereby tilt the O . . H vector away from the Al-rich site. Giese further notes that there are two categories of hydroxyls in amesite-$2H_2$:

(1) those in which the coordinating Al and the acceptor oxygen are on opposite sides of the OH [*e.t.* OH(2) and OH(4) in Fig. 3], and
(2) those in which the coordinating Al and the accep-

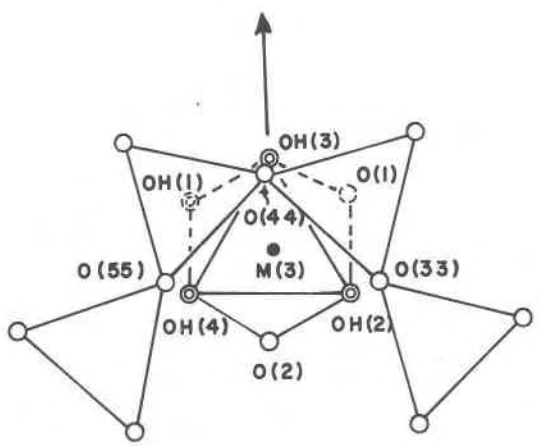

Fig. 3. Arrow shows approximate direction of major interlayer offset in Antarctic amesite-$2H_2$. Relationship of this direction to the structure is discussed in the text.

tor oxygen are on the same side of the OH [*e.g.* OH(3) in Fig. 3].

Giese shows that the combination of repulsion by octahedral Al of the same layer with attraction by the acceptor oxygen of the adjacent layer should cause the category 1 and category 2 hydroxyls to assume distinctly different orientations.

As seen in Figure 3, octahedral Al in site M(3) repels the H ion of the category 2 hydroxyl OH(3) directly away from its acceptor oxygen O(44). In contrast, M(3) repels the H ion of a category 1 hydroxyl in a direction that has only a component directed toward its acceptor oxygen. It is reasonable, therefore, that the entire plane of acceptor oxygens is offset in the same direction as the category 2 hydroxyl, as is shown by the centroid analysis, so that interlayer bonds of comparable efficiency are achieved. Without this offset, it seems likely that the bond involving the category 2 hydroxyl would be significantly less efficient than the other two.

This basic analysis also holds for the minor interlayer offsets, but it only predicts the general directions of offset. The analysis predicts a minor interlayer offset along $+X_2$ and $-X_3$ in Antarctic and Urals amesites respectively. The observed offsets, however, deviate by several degrees from the predicted directions and are best described as along $-Y_3$ and $+Y_1$ in Antarctic and Urals amesites respectively.

One possible explanation for the difference in magnitude of the major and minor interlayer offsets is that the orientation of the corrugation of the plane of surface hydroxyls relative to the direction of movement is different in the two cases. In major offsets, the OH whose H ion is repelled directly away from its acceptor oxygen (a category 2 hydroxyl) is also the most depressed hydroxyl. Thus, the acceptor oxygen that moves toward the category 2 hydroxyl also moves toward a depression in the plane of surface hydroxyls. In contrast, the category 2 hydroxyls involved in the minor interlayer offsets are not the most depressed. This suggests that the orientation of the corrugation of the surface hydroxyls has enhanced movement in the interlayers showing major offset, but has inhibited movement in the interlayers showing lesser offsets.

In summary, the ordered substitution of Al^{3+} for Mg^{2+} in the octahedral sites, which causes the H ions of the surface hydroxyls to be repelled away from the Al-rich sites, and the orientation of the corrugation of the plane of surface hydroxyl atoms significantly affect the direction and magnitude of interlayer offsets. The offsets determine the resultant direction of the Z axis and the values of the crystallographic alpha and beta angles.

Other structural features

The tetrahedra in this structure are rotated in the (001) plane by an average value of 14.7° so that the basal oxygens move toward the octahedral cations of the same layer. This is also the direction that will shorten the interlayer hydrogen bonds between the basal oxygens and the surface hydroxyls of the adjacent layer. The direction of tetrahedral rotation is the same as that found by Hall and Bailey for Antarctic amesite.

Steinfink and Brunton (1956, Fig. 6) present a diagram of their Urals structure that shows tetrahedral rotation in a direction opposite to that found in our study. Although their diagram represents a right-handed system, their atomic coordinates (see their Table 2) are left-handed. The actual direction of rotation indicated by their atomic coordinates in fact is the same as found in this study and by Hall and Bailey for Antarctic amesite.

Tetrahedral tilting combined with tetrahedral and octahedral ordering has displaced the tetrahedral apical oxygens and distorted the tetrahedral angles (Tables 3, 5). The tetrahedral sheet thicknesses are comparable to those of many other layer silicates.

Table. 5. Important structural features

α_{tet}(°)	Layer 1 : 14.7 Layer 2 : 14.7
τ_{tet}(°)	T(1) : 109.9 T(2) : 109.2 T(11) : 109.9 T(22) : 109.2
ψ_{oct}(°)	M(1) : 60.6 M(2) : 59.7 M(3) : 60.6 M(11) : 61.1 M(22) : 58.8 M(33) : 61.1
Sheet thickness (Å)	
tetrahedral	2.274
octahedral	2.017
Interlayer Separation	2.744

Tetrahedral rotation is calculated from $\alpha = 1/2[120° - \text{mean } O_b\text{-}O_b\text{-}O_b]$ *angle.*

Tetrahedral angle is defined as $\tau = O_{ap}\text{--}T\text{--}O_b$. *The ideal value is 109.47°.*

Mean octahedral angle is calculated from $\cos \psi = \text{oct. thickness}/2(M\text{--}O,OH)$.

The octahedral thicknesses, on the other hand, are unusually small and are comparable to those in dioctahedral dickite and nacrite. All of the octahedra are flattened, as indicated by the ψ values in Table 5, and the two large octahedra in each layer are flattened most severely ($\psi = 60.6°$ and $61.1°$ for layers 1 and 2, respectively) in order to fit onto the smaller Al-rich octahedron ($\psi = 59.7°$ and $58.8°$ in layers 1 and 2, respectively). An undistorted octahedron would have $\psi = 54.7°$. The combination of thin octahedral sheets and short interlayer separations leads to a total layer thickness of only 7.03Å. The statistics above agree closely with those reported for Antarctic amesite.

Theoretical ordering patterns

The ordering patterns of the Urals and Antarctic amesites are different. In order to account for the sector twinning observed in each specimen, five additional ordering patterns for Antarctic amesite and two additional ordering patterns for Urals amesite have been postulated to exist. These additional ordering patterns are generated by operating the 6_3 axis of the ideal space group on the two initial patterns.

The $2H_2$ structure also permits the possibility of other ordering patterns. There are two unique tetrahedral sites and three equivalent octahedral sites in each of the two layers. The chemical composition requires that one tetrahedral site and one octahedral site of each layer be Al-rich for an ordered structure. These restrictions permit 36 possible ordered structures, all of which exhibit local charge balance between layers.

Because of the pseudo-hexagonal nature of the amesite-$2H_2$ structure, not all of the 36 possible ordering patterns are unique. In the ordering patterns found for the Urals and Antarctic specimens, the (001) projection of the line defined by the octahedral Al cations is parallel to true X and this line intersects higher layers in the $-X$ direction (Fig. 1).

Because octahedral ordering has been shown to be a significant cause of the distortion that creates a triclinic true X and true Y from the ideal hexagonal configuration, similar alignments of octahedral Al along true X can be expected in the other unique patterns. Inspection of the $2H_2$ structure reveals that this alignment of octahedral Al occurs only if Al occupies either M(3) and M(11), or M(2) and M(22), or M(1) and M(33). In the 36 possible ordering patterns, there are only seven patterns whose octahedral cations occupy one of these three sets of sites. The remaining patterns can be generated by operating the 6_3 axis of the ideal space group on each of these seven patterns.

(1) T(2)–M(2)–T(22)–M(22) (Urals)
(2) T(2)–M(3)–T(11)–M(11) (Antarctic)
(3) T(1)–M(2)–T(11)–M(22)
(4) T(1)–M(3)–T(22)–M(11)
(5) T(1)–M(2)–T(22)–M(22)
(6) T(2)–M(1)–T(22)–M(33)
(7) T(1)–M(3)–T(11)–M(11)

The relative stabilities of the seven possible unique amesite-$2H_2$ structures probably depend on the orientation of distortions within the layers of these structures. We noted in the section discussing the beta angle that there is a relative offset of octahedral and tetrahedral Al from their ideal positions. The direction of offset is found to be parallel for both layers of an individual structure, and we assume that stability will be enhanced if the distortions in adjacent layers are oriented so that the layers fit together well. If the direction of Al cation offset is predicted for both layers of each of the seven unique structures above, using the criteria established in the section discussing the beta angle, the only ordering patterns in which the offsets are parallel for both layers are those in the Urals specimen, the Antarctic specimen, and the pattern T(1)–M(2)–T(11)–M(22). These are probably the three most stable arrangements.

Conclusions

Once a particular cation ordering pattern has been established for any mineral, it is customary to assume that all specimens of that mineral will have the same ordering pattern provided the environments of crystallization are similar. That is not the case for amesite-$2H_2$, where two different ordering patterns show equally good local charge balance. A second structure of the same amesite polytype normally would not have been attempted, but was considered necessary in this case in order to resolve the conflicting evidence provided by its optics, twinning, and infrared spectra. This study indicates that the infrared spectra of amesite require reinterpretation. It may be prudent also to examine the geometry of other crystal structures to see if alternative ordering patterns are both possible and crystallochemically plausible. This applies particularly to structures involving ordering in subgroup symmetry.

Acknowledgments

This research was supported in part by NSF grant EAR78-05394 (Earth Sciences Section), and in part by the Petroleum Re-

search Fund, administered by the American Chemical Society, PRF grants 8425-AC2 and 11224-AC2. Crystals of the Saranovskoye amesite were provided by the Smithsonian Institution.

References

Bailey, S. W. (1963) Polymorphism of the kaolin minerals. American Mineralogist, 48, 1196–1209.

Bailey, S. W. (1969) Polytypism of trioctahedral 1 : 1 layer silicates. Clays and Clay Minerals, 17, 355–371.

Giese, R. F., Jr. (1980) Hydroxyl orientations and interlayer bonding in amesite. Clays and Clay Minerals, 28, 81–86.

Hall, S. H. and Bailey, S. W. (1979) Cation ordering pattern in amesite. Clays and Clay Minerals, 27, 241–247.

Hall, S. H., Guggenheim, S., Moore, P., and Bailey, S. W. (1976) The structure of Unst-type 6-layer serpentines. Canadian Mineralogist, 14, 314–321.

Serna, C. J., Velde, B. D. and White, J. L. (1977) Infrared evidence of order–disorder in amesites. American Mineralogist, 62, 296–303.

Steinfink, H. and Brunton, G. (1956) The crystal structure of amesite. Acta Crystallographica, 9, 487–492.

Manuscript received, June 16, 1980;
accepted for publication, July 24, 1980.